Contribution from the Division of Chemistry,
National Research Council of Canada, Ottawa, Ontario, Canada K1A 0R9

EPR and FTIR Spectroscopic Study of the Reaction of Rhodium Atoms with CO in a Rotating Cryostat: Formation of $Rh(CO)_4$, $Rh_2(CO)_8$, and $Rh_4(CO)_{12}$[1]

J. H. B. Chenier, M. Histed,[2a] J. A. Howard,* H. A. Joly,[2b] H. Morris,[2a] and B. Mile*

Received January 13, 1988

Reaction of ground-state rhodium atoms with CO in hydrocarbon matrices at 77 K gives a mononuclear paramagnetic product, $Rh(CO)_4$, and a dinuclear diamagnetic product, $Rh_2(CO)_8$. There is no evidence for the presence of mononuclear Rh species with less than four CO ligands. Annealing of the samples leads to conversion of the monomer to the dimer and then to the tetramer, $Rh_4(CO)_{12}$. $Rh(CO)_4$ is an axially symmetric species with the magnetic parameters $a_{\parallel}(Rh) \leq 15$ MHz, $a_{\perp}(Rh) = 24$ MHz, $a_{\parallel}(C) = 47.8$ MHz, $a_{\perp}(C) = 36.4$ MHz, $g_{\parallel} = 2.0150$, and $g_{\perp} = 2.0020$. In marked contrast to the EPR spectrum of the congener $Co(CO)_4$, equal hyperfine interactions with four equivalent CO ligands are seen. The EPR parameters are consistent with a $^2B_2$ ground state in D_{2d} symmetry with the unpaired electron at Rh occupying the $d_{x^2-y^2}$ orbital; i.e., $Rh(CO)_4$ is slightly distorted from tetrahedral geometry. $Rh(CO)_4$ in two trapping sites shows infrared absorptions of the CO ligands at 2020 and 2009 cm^{-1}, while $Rh_2(CO)_8$ and $Rh_4(CO)_{12}$ have absorptions at 2086, 2061, 1860, and 1841 cm^{-1} and 2071, 2045, and 1878 cm^{-1}, respectively. FTIR spectra of mixed $^{13}CO/^{12}CO$ $Rh(CO)_4$ isotopomers are consistent with the D_{2d} structural assignment.

Introduction

Reaction of rhodium metal with CO was first studied by Hieber and Lagally,[3] who reported the formation of dirhodium octacarbonyl at high CO pressures and temperatures (460 atm, 473 K). This compound was subsequently prepared by Whyman[4,5] by subjecting liquid-paraffin-heptane solutions of $Rh_4(CO)_{12}$ to high pressures of CO (~430 atm) at lower temperatures (~254 K). He found that this dinuclear carbonyl was unstable under normal conditions of temperature and pressure and disproportionated to bridge-bonded tetrarhodium dodecacarbonyl

$$2Rh_2(CO)_8 \rightarrow Rh_4(CO)_{12} + 4CO \quad (1)$$

$Rh_2(CO)_8$ was also prepared by Hanlan et al.[6,7] by condensing high fluxes of Rh atoms into a pure CO matrix at 15 K. It was suggested that at this temperature the dinuclear carbonyl was formed by reaction of mononuclear rhodium carbonyls with Rh atoms and CO

$$Rh + CO \rightarrow Rh(CO)_n \xrightarrow{Rh,\ CO} Rh_2(CO)_8 \quad (2)$$

where $n = 1$-4 because only Rh and CO were mobile on solid CO. However, upon annealing, $Rh_2(CO)_8$ could have been formed by dimerization of $Rh(CO)_4$. $Rh_2(CO)_8$ disproportionated under dynamic vacuum conditions to bridge-bonded $Rh_4(CO)_{12}$ at ~225 K, and there was no evidence for nonbridged $Rh_2(CO)_8$.

At low concentrations of metal, monorhodium tetracarbonyl was the principle product,[8,9] and at low concentrations of CO in rare gas matrices, the coordinatively unsaturated mononuclear carbonyls $Rh(CO)_3$, $Rh(CO)_2$, and RhCO were identified.[8] The geometries of all four mononuclear rhodium carbonyls are in doubt although RhCO and $Rh(CO)_2$ appear linear whereas $Rh(CO)_3$ can have either planar (D_{3h} and C_{2v}) or nonplanar (C_{3v}) structures. $Rh(CO)_4$ is an interesting molecule because as a d^9 species a regular tetrahedral (T_d) geometry would have an orbitally degenerate ground state ($^2T_2$) and would be expected to undergo a C_{3v} or D_{2d} distortion to lift this degeneracy because of the Jahn-Teller theorem.[10] Infrared and optical spectra of $Rh(CO)_4$ are consistent with an approximately tetrahedral geometry or a slight C_{3v} distortion whereas the cobalt congener $Co(CO)_4$ undergoes a marked C_{3v} distortion.[11] However, even in the case of $Co(CO)_4$, Ozin and co-workers[12] had difficulty distinguishing the D_{2d} and C_{3v} structures unambiguously despite their careful examination of mixed isotopic CO systems, and indeed they speculated that both isomers were present in an argon matrix. It therefore seemed worthwhile to undertake an electron paramagnetic resonance (EPR) study alongside an infrared examination of matrix-isolated $Rh(CO)_4$ in an attempt to provide a more definitive structural assignment.

EPR spectral data of the phosphorus analogues, $Rh(PX_3)_4$, are conflicting. George et al.[13] concluded that $Rh[P(OPr^i)_3]_4$ has a tetragonally compressed tetrahedral structure (D_{2d}), while Pilloni et al.[14] suggested a square-planar geometry for the same molecule although they found that $Rh[P(Ph)_3]_4$ is tetragonally distorted.

Several rhodium carbonyl species are known to be involved in both homogeneous and heterogeneous catalysis by rhodium[15-18] so that there are commercial reasons for attempting to elucidate their structures.

Experimental Section

The rotating cryostat and furnace used to study the reactions of rhodium atoms with CO in inert hydrocarbon matrices have been described previously.[19] Rhodium was evaporated from a tungsten wire ($d = 0.030$ in.) clamped between the electrodes of the furnace. The rhodium melted to give a hanging drop in the center of the W wire. X-Band EPR spectra were obtained on Varian E-4 and E-12 and Bruker ESP 300 instruments equipped with a Systron-Donner Model 6054 microwave frequency counter and a Bruker Model ER 035 proton magnetometer. Temperature control was achieved with an Oxford Instruments ESR 9 liquid-helium cryostat and a cold-nitrogen-gas controller. Q-Band spectra were obtained on the Bruker ESP 300 machine using an ER 053 QRD microwave bridge and an ER 5102 QTN cavity. The frequency and magnetic field calibrations at the Q-band were performed with samples calibrated at the X-band. In situ IR spectra of deposits on the drum of the cryostat were obtained on a Mattson Sirius 100 FTIR spectrometer as described previously.[20] They were recorded initially at 77 K and then

(1) Issued as NRCC No. 30639.
(2) (a) Department of Chemistry and Biochemistry, Liverpool Polytechnic, Liverpool, England L3 3AF. (b) NSERC Postdoctorate Fellow, 1988.
(3) Hieber, W.; Lagally, H. *Z. Anorg. Chem.* **1943**, *251*, 96-113.
(4) Whyman, R. *J. Chem. Soc., Chem. Commun.* **1970**, 1194-1195.
(5) Whyman, R. *J. Chem. Soc., Dalton Trans.* **1972**, 1375-1381.
(6) Hanlan, L. A.; Ozin, G. A. *J. Am. Chem. Soc.* **1974**, *96*, 6324-6329.
(7) Hanlan, A. J. L.; Ozin, G. A.; Gray, H. B. *Inorg. Chem.* **1979**, *18*, 1790-1792.
(8) Ozin, G. A.; Hanlan, A. J. L. *Inorg. Chem.* **1979**, *18*, 2091-2100.
(9) Lever, A. B. P.; Ozin, G. A.; Hanlan, A. J. L.; Power, W. J.; Gray, H. B. *Inorg. Chem.* **1979**, *18*, 2088-2090.
(10) Jahn, H. A.; Teller, E. *Proc. R. Soc. London, Ser. A* **1937** *161*, 220-233.
(11) Crichton, O.; Poliakoff, M.; Rest, A. J.; Turner, J. J. *J. Chem. Soc., Dalton Trans.* **1973**, 1321-1324.
(12) Hanlan, L. A.; Huber, H.; Kündig, E. P.; McGarvey, B. R.; Ozin, G. A. *J. Am. Chem. Soc.* **1975**, *97*, 7054-7068.
(13) George, G. N.; Klein, S. I.; Nixon, J. F. *Chem. Phys. Lett.* **1984**, *108*, 627-630.
(14) Pilloni, G.; Zotti, G.; Zecchin, S. *J. Organomet. Chem.* **1986**, *317*, 357-362.
(15) Poels, E. K.; Ponec, V. *Catalysis (London)* **1983**, *6*, 196-205.
(16) Solymosi, F.; Tombacz, I.; Koszta, J. *J. Catal.* **1985**, *95*, 578-586.
(17) Gelin, P.; Lefebvre, F.; Ellench, B.; Naccache, C.; Ben Taarit, Y. In *Intrazeolite Chemistry*; Stucky, G. D., Dwyer, F. G., Eds.; ACS Symposium Series 218; American Chemical Society: Washington, DC, 455-464.
(18) Sayari, A.; Morton, J. R.; Preston, K. F. *J. Chem. Soc., Faraday Trans. 1*, **1988**, *84*, 413-431.
(19) Buck, A. J.; Howard, J. A.; Mile, B. *J. Am. Chem. Soc.* **1983**, *105*, 3381-3387.

0020-1669/89/1328-4114$01.50/0 Published 1989 by the American Chemical Society

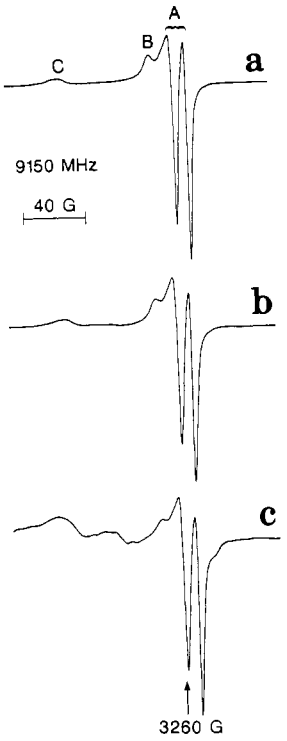

Figure 1. X-Band EPR spectra of Rh atoms and CO in adamantane at 77 K at CO inlet pressures of 0.5 Torr of CO (a), 0.0025 Torr of CO (b), and 0.00025 Torr of CO (c).

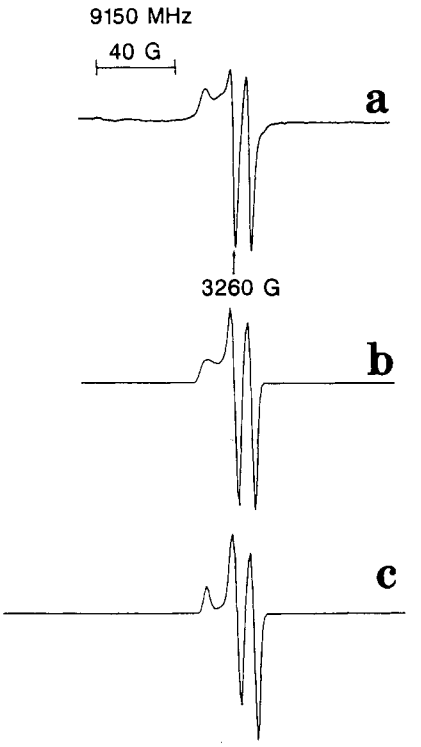

Figure 2. X-Band EPR spectrum of Rh atoms and CO in adamantane at 77 K after annealing to 173 K for 30 min (a) and computer simulated spectra using the parameters given in the text (b and c).

at higher tempertaures by warming the deposits on the drum of the cryostat. If major changes in the spectrum occurred at higher temperatures, the cryostat was recooled to 77 K and the spectrum rerecorded at this temperature. Spectra were the average of 256 scans at 4-cm^{-1} resolution from 4000 to 400 cm^{-1}, and the absorption spectrum of the matrix was usually subtracted from the matrix/Rh/CO spectrum.

Rhodium metal in the form of wire was obtained from Alfa Products, Danvers, MA. Carbon monoxide (99.99%) and ^{13}CO enriched to 99.9 atom % in ^{13}C were obtained from Matheson and Merck Sharpe and Dohme Ltd., Montreal, Canada, respectively. The inert matrices used were adamantane, cyclohexane, and perdeuteriocyclohexane.

Results

EPR. The EPR spectrum given by Rh atoms ($I = {}^1/_2$) and CO (0.5 Torr) in adamantane at 77 K (Figure 1a) was dominated by two derivative-shaped features (A) centered at $g = 2.0020$ with a spacing of 8.5 G and two absorptive features (B and C) centered at $g = 2.015$ and 2.053. Similar spectra were obtained at lower inlet pressures of CO (Figure 1b,c), but extra, rather broad features appeared in the spectrum at the lowest CO pressure that were also present in deposits containing only Rh and adamantane. These were probably transitions from rhodium clusters, but they are too poor in quality to justify further analysis at present.

The spectrum shown in Figure 2a was obtained after annealing a Rh/CO/adamantane deposit, prepared at 77 K, on the drum of the cryostat to 173 K and recooling to 77 K before removing the deposit for examination by EPR spectroscopy. The absorptive feature C was absent from this spectrum, while feature B remained together with the derivative features A, which were more nearly equal in intensity, possibly indicating the presence of a derivative line or lines associated with C in the preannealed sample. The paucity of data on C makes it inappropriate to suggest an assignment. A simulated spectrum of features A and B using the magnetic parameters $a_{\parallel}(Rh) = 0$ MHz, $a_{\perp}(Rh) = 24$ MHz, $g_{\parallel} = 2.015$, and $g_{\perp} = 2.0020$ was similar to the experimental spectrum (Figure 2b), suggesting that the carrier of the spectrum had axial symmetry. The absence of a Rh hyperfine interaction in the parallel direction was, however, not unambiguous because simulations using $a_{\perp}(Rh) = 24$ MHz, $g_{\perp} = 2.0020$, $a_{\parallel}(Rh) =$ 25–36.5 MHz, $g_{\parallel} = 2.0110$–2.012 and line widths of 5 MHz gave almost as good a fit with the experimental spectrum (see, e.g., Figure 2c).

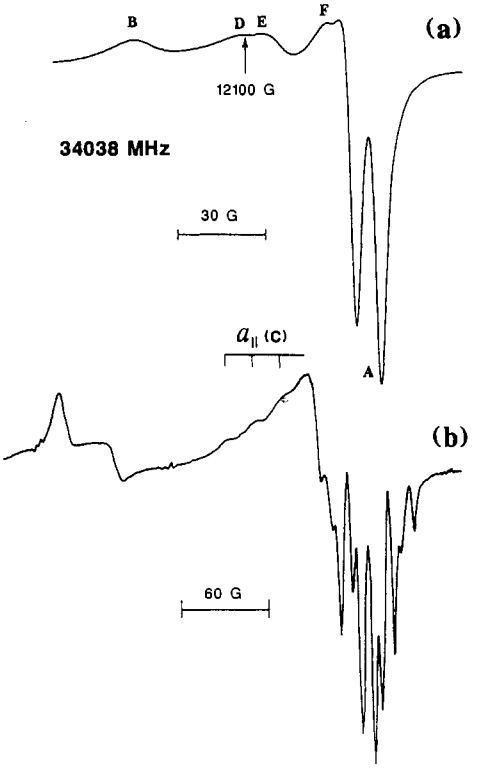

Figure 3. Q-Band spectra of Rh atoms and CO (a) or ^{13}CO (b) in adamantane at 96 K at a CO inlet pressure of 0.5 Torr.

The spectrum at the higher frequency of the Q-band ($\nu \sim 34$ GHz), which increases the field separation of features with different g factors but unfortunately gives broader lines, revealed the presence of three additional transitions between B and A labeled D, E, and F in Figure 3a. Taking B as the low-field component and each of these transitions in turn as the high-field

(20) Howard, J. A.; Sutcliffe, R.; Hampson, C. A.; Mile, B. *J. Phys. Chem.* **1986**, *90*, 4268–4273.

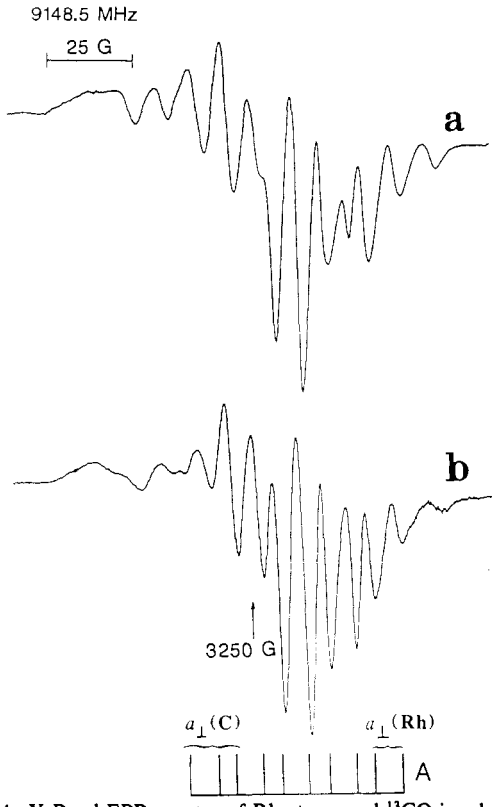

Figure 4. X-Band EPR spectra of Rh atoms and ^{13}CO in adamantane at 77 K (a) and after annealing to 173 K for 30 min (b). The stick spectrum denotes the 10 perpendicular features of $Rh(^{13}CO)_4$.

component of the Rh parallel hyperfine interaction gave $a_\parallel$(Rh) = 104 MHz and $g_\parallel$ = 2.0124, $a_\parallel$(Rh) = 124 MHz and $g_\parallel$ = 2.0120, and $a_\parallel$(Rh) = 184 MHz and $g_\parallel$ = 2.010, respectively. However, none of these analyses gave an acceptable simulation of the X-band spectrum, and they can therefore be discounted. In addition there were no features in the Q-band spectra that could be assigned to the $M_I = -^1/_2$ component of a doublet with $a_\parallel$(Rh) = 25–36.5 MHz. The Q-band spectrum was therefore only consistent with $a_\parallel$(Rh) $\leq$ 15 MHz, the width of the X-band parallel feature.

When the sample was annealed in the cavity of the Q-band spectrometer, the resolution of feature A was lost at 115 K and the signal intensity decreased rapidly above this temperature. Broad parallel and perpendicular features, $g_\parallel$ = 2.0338 and $g_\perp$ = 2.008, developed at 145 K and coalesced at 220 K to give a broad singlet at g = 2.028, which had the appearance of a conduction EPR spectrum with an assymmetry parameter (positive peak height/negative peak height) of ~1.3. When the sample was recooled to 94 K, features A reappeared with almost the original intensity.

Reaction of Rh atoms with ^{13}CO in adamantane gave a multilined spectrum (Figure 4a) that was dominated by 10 derivative (i.e., perpendicular) features with $a_\perp$(C) = 36.4 MHz, suggesting that the carrier of the spectrum contained four equivalent or nearly equivalent carbon nuclei. The spectrum resolved and simplified on annealing to 173 K (Figure 4b), and five doublets were resolved with $a_\perp$(Rh) = 24 MHz and $a_\perp$(C) = 36.4 MHz, proving that the spectrum could be assigned to rhodium tetracarbonyl, $Rh(^{13}CO)_4$. In this spectrum the parallel features were either completely masked by the perpendicular features or were too broad to detect. The perpendicular features of the EPR spectrum of $Rh(^{13}CO)_4$ were better resolved at 5.3 K (Figure 5a) and indicated the presence of a second less intense quintet of doublets D with larger Rh and ^{13}C hfi (hyperfine interaction) values. This was confirmed by subtracting the annealed spectrum from the 77 K spectrum, which left the quintet of doublets from a second carrier as shown in Figure 5b with $a_\perp$(Rh) = 27.5 MHz and $a_\perp$(C) = 64.5 MHz. These results tentatively suggest the presence of a second less abundant rhodium

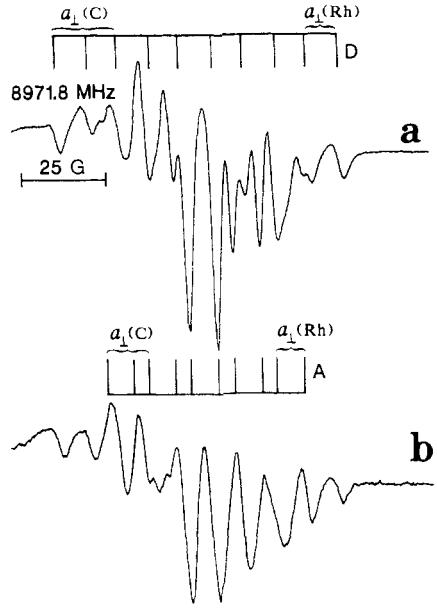

Figure 5. X-Band EPR spectra of $Rh/^{13}CO$/adamantane at 5.3 K (a) and after subtracting the spectrum of an annealed sample from one that had not been annealed (b). The stick spectrum D refers to both spectra.

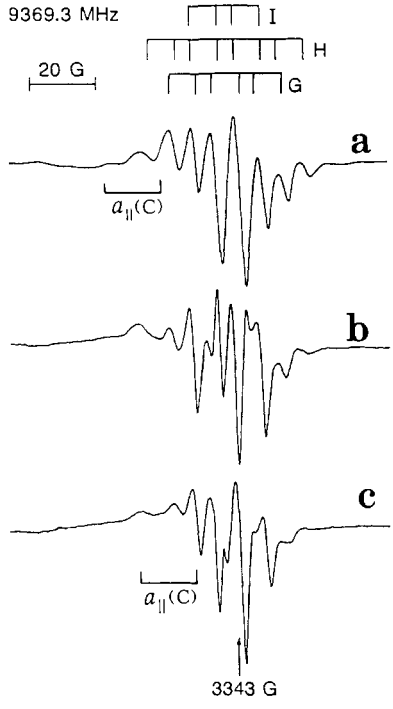

Figure 6. X-Band EPR spectra of Rh atoms and mixtures of ^{13}CO and ^{12}CO containing 50% (a) 20% (b) and 10% (c) ^{13}CO. Spectra b and c have had the spectrum of $Rh(CO)_4$ subtracted from the original spectrum.

tetracarbonyl that is possibility $Rh(CO)_4$ in a second, less stable trapping site. Further analysis was, however, not attempted because we could not determine $a_\parallel$(Rh) and $a_\parallel$(C).

In order to prove the presence of four magnetically equivalent or nearly equivalent CO ligands, $Rh(CO)_4$ was prepared from mixtures of ^{12}CO and ^{13}CO containing 10, 20, and 50% ^{13}CO. The spectra obtained from these mixtures are shown in Figure 6 and they are all consistent with four equivalent or nearly equivalent ligands. Statistically the mixture of ^{12}CO and ^{13}CO in the ratio 1:1 should give 37.5% $Rh(^{13}CO)_2(^{12}CO)_2$, 25% $Rh(^{13}CO)(^{12}CO)_3$, 25% $Rh(^{13}CO)_3(^{12}CO)$, 6.25% $Rh(^{13}CO)_4$ and 6.25% $Rh(^{12}CO)_4$. The spectrum from this mixture (Figure 6a) is a composite spectrum made up predominantly of contributions from a triplet of doublets (G) from $Rh(^{13}CO)_2(^{12}CO)_2$, a quartet of doublets (H) from $Rh(^{13}CO)_3(^{12}CO)$, and a doublet of doublets

(I) from $Rh(^{13}CO)(^{12}CO)_3$ with a ^{13}C hfi of 36.4 MHz. The mixture of $^{13}CO/^{12}CO$ in the ratio 1:5 should give 41% $Rh(^{13}CO)(^{12}CO)_3$, 41% $Rh(^{12}CO)_4$, 15.4% $Rh(^{13}CO)_2(^{12}CO)_2$, 2.5% $Rh(^{13}CO)_3(^{12}CO)$, and 0.16% $Rh(^{13}CO)_4$, and the spectrum obtained from this mixture (Figure 6b) after subtraction of the spectrum from $Rh(^{12}CO)_4$ is clearly dominated by a doublet of doublets (I) with $a_\perp(C) = 36.4$ MHz and $a_\perp(Rh) = 24$ MHz from $Rh(^{13}CO)(^{12}CO)_3$. A mixture of ^{13}CO and ^{12}CO in the ratio 1:10 should give 65.1% $Rh(^{12}CO)_4$, 29.1% $Rh(^{13}CO)(^{12}CO)_3$, 4.7% $Rh(^{13}CO)_2(^{12}CO)_2$, 0.4% $Rh(^{13}CO)_3(^{12}CO)$, and 0.01% $Rh(^{13}CO)_4$. Spectral subtraction was not as successful in this case, but the resulting spectrum shown in Figure 6c certainly shows the presence of a doublet of doublets from $Rh(^{13}CO)(^{12}CO)_3$. The spectrum of $Rh(^{13}CO)(^{12}CO)_3$ was simple enough that some of the parallel features were resolved and gave $a_\parallel(C) = 47.6$ MHz. This value of $a_\parallel(C)$ was confirmed by analysis of the Q-band spectrum of $Rh(^{13}CO)_4$ (Figure 3b), which had 10 perpendicular features and three reasonably well-resolved parallel features with a spacing of 47.6 MHz centered at $g = 2.015$.

Spectra from Rh atoms and ^{12}CO and ^{13}CO in cyclohexane were similar to those in adamantane, and the magnetic parameters were identical within experimental error in the two hydrocarbon matrices.

FTIR. The FTIR spectrum given by Rh atoms and CO at an inlet pressure of 0.5 Torr in adamantane at 77 K after a deposition time of 2 min gave new bands at 2086, 2061, 2020, 2009, 1860, and 1841 cm^{-1} in the CO stretching region (2200–1700 cm^{-1}). The spectrum was similar to the one given by Rh atoms in solid CO[8] at a Rh to CO ratio of 1:100 except that the 2020-cm^{-1} band was less prominent relative to the 2009-cm^{-1} band in our spectrum. After 10 min of deposition the bands at 2086, 2061, 1860, and 1841 cm^{-1} had increased significantly in intensity relative to the 2020- and 2009-cm^{-1} bands. The four bands that increased in intensity with deposition time had frequencies similar to those of the bridged form of $Rh_2(CO)_8$[5,6] while the two bands at 2020 and 2009 cm^{-1} had frequencies similar to the two bands in solid CO and argon from $Rh(CO)_4$.[8] Ozin and Hanlan[8] found that the relative intensities of these two bands did not vary with experimental condition whereas we found that the relative intensities changed with inlet pressure of CO but not in any consistent manner. We concluded that they arose from $Rh(CO)_4$ in two slightly different trapping sites in agreement with the EPR results.

When the sample was annealed at 163 K and recooled at 77 K, the bands assigned to $Rh_2(CO)_8$ remained virtually unchanged in intensity whereas the bands assigned to $Rh(CO)_4$ decreased 3-fold in intensity similar to the decrease in intensity of the EPR transitions assigned to $Rh(CO)_4$ over the same temperature range. This confirmed that they can be assigned to this species in agreement with Ozin and Hanlan.[8]

Lowering the CO inlet pressure to 2.5×10^{-3} Torr gave a similar spectrum with all six bands readily resolved while lowering the pressure still further to 2.5×10^{-4} Torr produced a spectrum with only the two bands from $Rh(CO)_4$.

Reaction of Rh atoms with ^{13}CO in adamantane at 77 K gave an FTIR spectrum in which the bands assigned to $Rh(CO)_4$ and $Rh_2(CO)_8$ were shifted to lower frequency by ~45 cm^{-1} and a 1:1 mixture of ^{12}CO and ^{13}CO gave a pattern of lines between 2009 and 1964 cm^{-1}, which was consistent with a tetracarbonyl.[21] The resolution was, however, not good enough to allow a meaningful estimate to be made of the ratio $k_{CO}/k_{CO:CO}$ between the stretching force constant and the interaction constant.

Further annealing of deposits containing $Rh_2(CO)_8$ to 200 K caused spectral changes that could be interpreted in terms of formation of tetrarhodium dodecacarbonyl.[4,5] Thus bands at 2086 and 2061 cm^{-1} disappeared and were replaced by a strong band at 2071 cm^{-1} with a shoulder at 2045 cm^{-1}. The rather broad bridging-CO band also moved to higher frequency at 200 K as observed by Whyman[4,5] for the transformation of $Rh_2(CO)_8$ to $Rh_4(CO)_{12}$.

(21) Darling, J. H.; Ogden, J. S. *J. Chem. Soc., Dalton Trans.* **1972**, 2496–2503.

Discussion

EPR and FTIR spectroscopic studies of the products given by reaction of Rh atoms with CO on a solid hydrocarbon surface at 77 K indicate the formation of two major products, the paramagnetic monorhodium tetracarbonyl, $Rh(CO)_4$, and the diamagnetic bridge-bonded dirhodium octacarbonyl $Rh_2(CO)_8$. There is no evidence for the coordinatively unsaturated mononuclear carbonyls $Rh(CO)_3$, $Rh(CO)_2$, and RhCO even at the lowest CO inlet pressure.

The structure of $Rh(CO)_4$ is of theoretical interest because it is a congener of cobalt tetracarbonyl, $Co(CO)_4$, which has a $^2A_1$ ground state in C_{3v} symmetry.[11] The EPR spectrum of $Co(CO)_4$ is consistent with this assignment because it shows one unique large ^{13}C hyperfine interaction and three small and equivalent ^{13}C hyperfine interactions.[12,22,23] It is immediately apparent from the present work that $Rh(CO)_4$ is not isostructural with $Co(CO)_4$ because the four CO ligands are magnetically equivalent or nearly equivalent. We first discuss the analysis of the EPR spectra of $Rh(CO)_4$.

EPR Spectral Analysis. The observation that $|g_\parallel| > |g_\perp| \sim 2.0023$ for $Rh(CO)_4$ suggests that the unpaired electron at Rh occupies the $4d_{x^2-y^2}$ orbital whereas $Co(CO)_4$ has $|g_\perp| > |g_\parallel| \sim 2.0023$ and a large d_{z^2} orbital contribution to the SOMO.[24]

If we assume that $g_\perp$ and $g_\parallel$ are both positive, the observed values of $\Delta g_\parallel$ and $\Delta g_\perp$ ($\Delta g_\parallel = g_\parallel - 2.0023$) for $Rh(CO)_4$ are small. The positive value of $\Delta g_\parallel$ (0.0127) indicates some spin–orbit coupling between the ground-state $d_{x^2-y^2}$ orbital and the filled d_{xy} orbital. The formulas for $g_\parallel$ and $g_\perp$ to the first order in λ/Δ for a $d_{x^2-y^2}$ orbital of a d^9 ion, where λ, the spin–orbit parameter for Rh,[25] is 968 cm^{-1}, are

$$g_\parallel = 2.0023 + 8\lambda/\Delta_0$$

$$g_\perp = 2.0023 + 2\lambda/\Delta_1$$

and Δ_0 and Δ_1 are the energy separations of the $d_{x^2-y^2}$ and d_{xy} orbitals and the $d_{x^2-y^2}$ and d_{xz} and d_{yz} orbitals, respectively. Since $g_\perp \sim 2.0023$ and $g_\parallel = 2.0150$ both Δ_1 and Δ_0 are very large. The low Δg values could also partly result from contributions of the nominally empty 5p oribitals to the SOMO since this would produce a negative shift of g.

The rhodium hyperfine interactions are of interest because they are rarely observed for rhodium(0) species. They have a maximum value when the external field is directed along the axis in which the g value is a minimum, i.e., perpendicular to the $d_{x^2-y^2}$ orbital.

An unpaired electron in a $d_{x^2-y^2}$ orbital generates anisotropy of the form $-^4/_7P$, $^2/_7P$, and $^2/_7P$, where P is the anisotropic hyperfine interaction. If the isotropic interaction is generated solely by core polarization it would be negative and the net principal hyperfine interactions ($A_{iso} + 2A_{dip}$, $A_{iso} - A_{dip}$, and $A_{iso} - A_{dip}$) would be large, small, and small and not as we find for $Rh(CO)_4$—small, large, and large. A possible explanation of this apparent anomaly is direct population of the 5s orbital, which would result in a positive isotropic component.

The small value of $\Delta g_\parallel$ and $\Delta g_\perp$ suggest that orbital angular momentum is quenched and the isotropic and anisotropic hyperfine interactions are given by

$$P_{exptl} = {}^7/_6(a_\parallel - a_\perp)$$

$$A_{iso} = (a_\parallel + 2a_\perp)/3$$

Substituting the value of $|a_\parallel| = 0$–15 MHz and $|a_\perp| = 24$ MHz into these equations gives $|A_{iso}| = 8$–13 MHz and $|P_{exptl}| = 10.5$–45.5 MHz depending on whether $a_\parallel$ and $a_\perp$ are positive or

(22) Fieldhouse, S. A.; Fullam, B. W.; Neilson, G. W.; Symons, M. C. R. *J. Chem. Soc., Dalton Trans.*, **1974**, 567–569.
(23) Fairhurst, S. A.; Morton, J. R.; Preston, K. F. *J. Magn. Reson.* **1983**, *55*, 453–459.
(24) Abragam, A.; Bleaney, B. *Electron Paramagnetic Resonance of Transition Ions*; Claredon Press: Oxford, U.K., 1970; Chapter 7.
(25) Raynor, J. B.; Goodman, B. A. *Adv. Inorg. Chem. Radiochem.* **1970**, *13*, 136–341.

Table I. EPR Parameters for Group 9 Mononuclear Tetracarbonyls[a]

	$Co(CO)_4$			$Rh(CO)_4$
matrix	CO	krypton	adamantane	adamantane
$a_\parallel$(M)	174.3	174.9	183.7	<15
$a_\perp$(M)	−175.2	−166.0	−164.9	24
$a_\parallel$(C)	78.1 (1)[b]	75.8 (1)[b]	77.5[b]	47.8 (4)[b]
$a_\perp$(C)	−76.5 (1)[b]	−68.6 (1)[b]	−70.6 (1)[b]	36.4 (4)[b]
$g_\parallel$	2.007	2.0059	2.019	2.015
$g_\perp$	2.128	2.1299	2.123	2.002
ρ_d(M)	0.51	0.47	0.43	<0.4
ρ_s(M)	−0.01	~−0.01	~−0.04	~0.00
ρ_{2p}(C)	0.49 (1)[b]	0.47 (1)[b]	0.47 (1)[b]	0.03 (4)[b]
ρ_{2s}(C)	0.007 (1)[b]	−0.005 (1)[b]	−0.006 (1)[b]	0.010 (4)[b]

[a] Hyperfine interactions in MHz. [b] Numbers in parentheses indicate the number of carbon nuclei having the given hyperfine interaction.

negative. Dividing these values by the one-electron parameters A = 1229 MHz and P = 121 MHz for unit spin population in the 5s and 4d orbitals of Rh[26] gives s and d unpaired spin populations ρ_{5s} = 0.0065–0.01 and ρ_{4d} = 0.09–0.38. Although these unpaired spin population estimates are approximate, we can conclude that the Rh 5s orbital contribution to the SOMO is minimal. The d orbital contribution ρ_{4d} is lower than that in $Co(CO)_4$ where ρ_{3d} = 0.47.[23] This may be because there is some unfilled 5p orbital admixture into the SOMO of $Rh(CO)_4$ that would reduce P_{exptl} because its contribution is of opposite sign to that of the filled d orbitals. This would not be unusual since the low values of metal hyperfine interactions in other d^9 metal complexes are generally attributed to such admixture of p and d orbitals. This is in fact the explanation that has been suggested for the complete absence of a Rh hyperfine interaction in $Rh[P(OPr^i)_3]_4$.[13]

Turning to the ^{13}C hyperfine tensors, $|a_\parallel(C)|$ is $>|a_\perp(C)|$, and the sign of these interactions cannot be determined. Furthermore, the measured values may not be the principle ones but are the interactions along the principle directions of the **g** tensor. We can however conclude that the $2p_z$ orbitals are parallel to the z axis of the **g** tensor and $a_\parallel(C)$ is certainly a principle value. The p_x and p_y orbitals are at an angle of 45° to the x and y axes of the **g** tensor, but it would appear that $a_x(C) = a_y(C) = a_\perp(C)$ and the measured value is in fact the principle one.

If we assume that $a_\perp$ is negative as it is for $Co(CO)_4$,[23] the unpaired spin population in the C $2p_z$ orbital is calculated to be 0.26, which when multiplied by a factor of 4 gives an unacceptably large value of the total ligand unpaired spin population of 1.04. The alternative analysis with $a_\perp$ positive gives A_{iso} = 40.2 MHz and A_{dip} = 3.8 MHz, which when divided by A = 3777 MHz and αP = 107.4 MHz for ^{13}C gives ρ_{2s} = 0.01 and ρ_{2p} = 0.03.

The total unpaired spin population for $Rh(CO)_4$ is, therefore, estimated to be <0.55, which is acceptable considering the difficulties experienced in determining $a_\parallel$(Rh) and $a_\parallel$(C) and the usual inaccuracies involved in the calculation of unpaired spin populations and the possibility of both 5p and 4d orbital participation in the SOMO.

The magnetic parameters of $Rh(CO)_4$ in adamantane are presented in Table I along with those of $Co(CO)_4$ in CO,[12] krypton,[23] and adamantane.[27] It is worth noting that the magnetic parameters of $Co(CO)_4$ in adamantane are similar to those in CO and krypton although the parallel **a** and **g** tensors are significantly larger in the hydrocarbon. This is probably associated with a modification of the spin–orbit interaction by lattice vibrations, which is apparently more important in adamantane than it is in CO and krypton.

FTIR Spectral Analysis. The CO stretching vibrational frequencies for rhodium carbonyls prepared by metal vapor deposition techniques are summarized in Table II.

$Rh(CO)_4$ in adamantane gives rise to a strong and a weak band in the CO stretching region. Since the relative intensities of these

Table II. Infrared Absorptions for the Products of Reaction of Rh Atoms with CO in Matrices at Low Temperatures

species	matrix	ν/cm^{-1}	ref
RhCO	argon	2012.8/2008	8
$Rh(CO)_2$	argon	2014.6	8
$Rh(CO)_3$	argon	2018.4	8
$Rh(CO)_4$	CO	2020/2019; 2012/2010	8
	adamantane	2020/2009	*b*
$Rh_2(CO)_8$	argon	2060, 2043, 2038, 1852, 1830	6
	A[a]	2086, 2061, 1860, 1845	4
	adamantane	2086, 2061, 1860, 1841	*b*
$Rh_4(CO)_{12}$	A[a]	2076, 2071, 2045, 1886	4
	adamantane	2071, 2045, 1878	*b*

[a] A = liquid-paraffin–heptane mixture. [b] This study.

two bands varied with experimental conditions, they must be associated with two trapping sites and are not symmetric and asymmetric stretching modes of a markedly distorted C_{3v} or D_{2d} tetrahedral molecule. This is consistent with the observation of two distinct EPR spectra in adamantane.

It is interesting to note that bridge-bonded $Rh_2(CO)_8$ is formed under our experimental conditions at 77 K and that its concentration relative to $Rh(CO)_4$ increases with time. It could be formed by dimerization of mobile $Rh(CO)_4$ on the solid hydrocarbon surface but could also be formed by reaction of an isolated $Rh(CO)_4$ with a mobile Rh atom followed by reaction with CO.

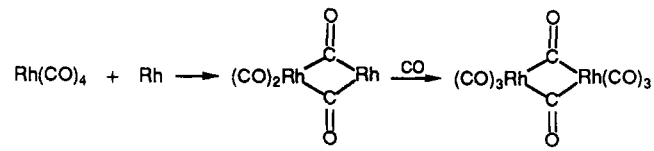

Our work provides further evidence that the bridge-bonded $Rh_2(CO)_8$ is unstable relative to $Rh_4(CO)_8$.

The apparent absence of FTIR evidence for coordinatively unsaturated mononuclear carbonyls suggests that they may be removed by rapid reaction with mobile Rh atoms on the cold hydrocarbon surface

$$Rh(CO)_n \xrightarrow{Rh} Rh_2(CO)_n \xrightarrow{CO} Rh_2(CO)_8$$

where n = 1–3.

Structure of $Rh(CO)_4$. It is clear from this work that $Rh(CO)_4$ has a structure different from that of $Co(CO)_4$ because it has a hyperfine interaction with four equivalent rather than one unique and three equivalent carbon nuclei and a significant $d_{x^2-y^2}$ rather than d_{z^2} orbital participation in the SOMO. EPR spectra assigned to $Co(^{13}CO)_4$ in argon are however somewhat ambiguous since in addition to the molecule with one unique ^{13}CO ligand there is one with two equivalent ^{13}CO ligands that Ozin et al.[12] assign to a D_{2d} molecule. However, Fairhurst et al.[23] suggest that the carriers of the spectra in Ar are the lower carbonyls CoCO, $Co(CO)_2$, and $Co(CO)_3$. Only C_{3v} $Co(CO)_4$ is observed in Kr[23] and adamantane.[27]

The starting point for discussing the 17-electron species $Rh(CO)_4$ is a regular tetrahedron with four equivalent CO ligands as found for 18-electron closed-cell species such as $Ni(CO)_4$ and $Pt(CO)_4$. Since the upper t_{2g} orbitals (d_{xy}, d_{zx}, and $d_{x^2-y^2}$) are degenerate in T_d symmetry the Jahn–Teller theorem[10] requires that the molecule distort to lift this degeneracy. $Co(CO)_4$ displays one type of distortion, a shortening or elongation of the Co–CO bond along the d_{z^2} axis. The other distortion is a squashing of the tetrahedron to give a molecule with D_{2d} symmetry which in the extreme case has a square-planar distribution of CO ligands in D_{4h} symmetry. Elian and Hoffmann[28] have examined such distortions in detail and concluded, together with Burdett,[29] that the D_{2d} distortion produces a slightly more stable structure than the C_{3v} distortion. A modified form of their energy diagram is shown in Figure 7. (Note that we have used the same coordinate

(26) Morton, J. R.; Preston, K. F. *J. Magn. Reson.* **1978**, *30*, 577–582.
(27) Histed, M.; Howard, J. A.; Mile, B. Unpublished results.
(28) Elian, M.; Hoffmann, R. *Inorg. Chem.* **1975**, *14*, 1058–1076.
(29) Burdett, J. K. *J. Chem. Soc., Faraday Trans. 2* **1974**, *70*, 1599–1613.

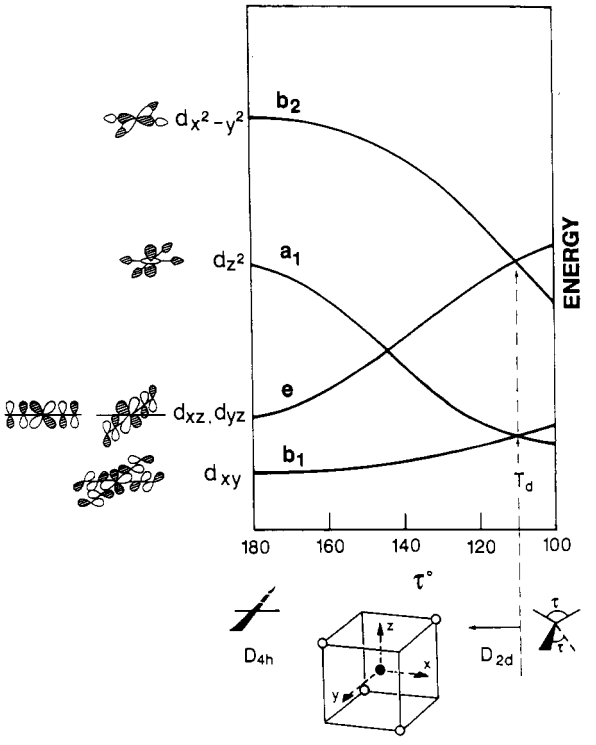

Figure 7. Energy levels of $Rh(CO)_4$ of D_{2d} symmetry as a function of the OCRhCO angle τ.

system as Elian and Hoffman,[28] which is rotated by 45° from the usual system with the result that the SOMO is $d_{x^2-y^2}$; the interactions with the sp^3 orbitals that result in a tetrahedral structure are not included for the sake of clarity. The standard coordinate system is used to describe the C_{3v} structure of $Co(CO)_4$ with the semioccupied d_{z^2} orbital directed toward the unique CO ligand). The distortion from the tetrahedral angle, $\tau > 109.5°$, places the unpaired electron in the b_2 orbital which is $d_{x^2-y^2}$ at rhodium and antibonding with the 5σ orbitals of the CO ligands. This designation is consistent with the EPR parameters of $Rh(CO)_4$.

It should however be noted that magnetic equivalence of the four CO ligands in the xy plane is not consistent with a large D_{2d} distortion because the unpaired spin population at carbon residing largely in the 2p orbital should lead to two sets of magnetically inequivalent though spatially equivalent ligands. Variable-temperature ESR studies support a slight distortion for $Rh(CO)_4$ because the signal disappears at temperatures above 120 K and returns upon recooling to 94 K.

The rather large value of the spin–orbit coupling constant of Rh (968 cm^{-1})[25] requires consideration of the nonapplication of the Jahn–Teller theorem and the persistence of the d^9 species in a tetragonal geometry because the spin–orbit coupling allows mixing of the d orbitals that in its absence are symmetry disallowed from mixing.[12,25] In effect the spin–orbit coupling results in a symmetric SOMO involving all the d orbitals. Thus the difference in the electrostatic interactions between the 5σ electrons of the CO and d orbitals containing one or two electrons does not arise, and hence the physical cause for the Jahn–Teller distortion is no longer extant (see ref 30 and 31 for a rigorous discussion of the effects of spin–orbit coupling on Jahn–Teller distortions). Thus in principle a regular tetrahedron structure in T_d symmetry is possible for $Rh(CO)_4$ because of spin–orbit coupling. The EPR data show that this is not the case since such a molecule would have isotropic g and A tensors. Even a cursory glance at Figure 1 shows that this is not so for $Rh(CO)_4$. The molecule must therefore distort to D_{2d} symmetry. However the quite small departure of the g and A values from isotropy show that the distortion is probably small, i.e., τ is close to 109.5°.

The different distortions of $Co(CO)_4$ and $Rh(CO)_4$ must involve different CRhC deformations but may also be related to the lower energy of the d^9 state in Rh (−7.05 eV) compared to that in Co (−4.45 eV), which results in a closer interaction of the Rh $4d_{x^2-y^2}$ orbital with 5σ orbitals of CO(−14.8 eV); the lower energy of the d orbitals in Rh is of course reflected in the different ground electronic states of Rh ($4d^85s^1$) and Co ($3d^74s^2$). It is possible that C_{3v} and D_{2d} structures lie close in energy, but the observation of only one isomer for $Co(CO)_4$ and $Rh(CO)_4$ in adamantane at temperatures up to 163 K indicates that they differ in energy by at least 5 kcal mol^{-1} or have energy barriers of this magnitude against such interconversion. It appears that $Rh(CO)_4$ is isostructural with $Rh[P(OPr^i)_3]_4$[13] and $Rh[P(Ph)_3]_4$,[14] which also have D_{2d} symmetry with the unpaired electron in a $d_{x^2-y^2}$ orbital at the metal center and equivalent hfi with the four phosphorus ligands. It will be of interest to study the cobalt congeners $Co[P(OPr^i)_3]_4$ and $Co[P(Ph)_3]_4$, which have only received cursory attention.[32,33]

In conclusion it is worth noting that $Rh(CO)_4$ is unique among Rh(0) complexes in that it exhibits a well-resolved Rh hyperfine interaction. This is different from Rh(0) complexes with trivalent phosphorus ligands, which only exhibit phosphorus hyperfine interactions.[34]

Acknowledgment. We thank NATO for a research grant (No. 442/82), Drs. J. R. Morton, K. F. Preston, and J. S. Tse for many helpful discussions, and Dr. R. Sutcliffe for some initial experiments on this system. M.H. thanks the SERC for the award of a CASE studentship and the ICI for collaboration on the project, and H.A.J. thanks the NSERC for a postdoctoral fellowship. We also thank the reviewers for many helpful suggestions.

Registry No. Rh, 7440-16-6; CO, 630-08-0; $Rh(CO)_4$, 28132-77-6; $Rh_2(CO)_8$, 29658-60-4; $Rh_4(CO)_{12}$, 19584-30-6; $Co(CO)_4$, 58207-38-8; $Rh(^{13}CO)_2(^{12}CO)_2$, 122676-86-2; $Rh(^{13}CO)_3(^{12}CO)$, 122676-87-3; $Rh(^{13}CO)(^{12}CO)_3$, 122676-88-4; $Rh(^{13}CO)_4$, 122676-89-5; ^{13}CO, 1641-69-6; adamantane, 281-23-2.

(30) Griffith, J. S. *The Theory of Transition-Metal Ions*, Cambridge University Press: Cambridge, England, 1961.
(31) Wertz, J. E.; Bolton, J. R. *Electron Spin Resonance: Elementary Theory and Practical Applications*; McGraw-Hill: New York, 1972.
(32) Klein, H.-F.; *Angew. Chem., Int. Ed. Engl.* **1980**, *19*, 362–375.
(33) Muetterties, E. L.; Bleeke, J. R.; Yang, Z.-Y.; Day, V. W. *J. Am. Chem. Soc.* **1982**, *104*, 2940–2942.
(34) Mueller, K. T.; Kunin, A. J.; Greiner, S.; Henderson, T.; Kreilick, R. W.; Eisenberg, K. *J. Am. Chem. Soc.* **1987**, *109*, 6313–6318.